Quantum Electronics **50** (6) 603–607 (2020)

LASER PLASMA

https://doi.org/10.1070/QEL17220

Soft X-ray and EUV emission spectra of beryllium plasma produced by neodymium-glass laser radiation with broad frequency and angular spectra

A.T. Sahakyan, S.N. Andreev, A.A. Kologrivov, T.T. Kondratenko, V.N. Puzyrev, A.N. Starodub, I.Yu. Tolstikhina, A.A. Fronya, O.F. Yakushev

Abstract. **We present the results of an experimental study of soft X-ray (SXR) and extreme ultraviolet emission spectra of the plasma produced by exposing a plane solid beryllium target to laser radiation with broad frequency and angular spectra. SXR lines up to 1s–9p of Be IV as well as the plasma continuum are recorded for a laser focal-spot intensity of 5.3×10^{13} W cm^{-2}. To model the SXR beryllium plasma spectra, simulations are carried out using the INDHAUS programme and the FLYCHK code in the framework of local thermodynamic equilibrium model, which agree nicely with experimentally obtained results.**

Keywords: *laser-produced plasma, beryllium, soft X-ray radiation, extreme ultraviolet radiation, local thermodynamic equilibrium.*

1. Introduction

At present, beryllium, despite its harmful properties, is widely employed in many scientific and technological tasks [1–15]. For instance, in laser fusion it is proposed to use beryllium in the making of the shells of targets intended for the ignition of fusion fuel [16–19]. From the standpoint of laser-plasma research, mention should be made of the possibility to use subcritical-density beryllium foam [11–13] as an auxiliary substance deposited in a thin layer on the main target material. The plasmas of the main material and beryllium foam will emerge practically simultaneously, and the hydrodynamic wave of the beryllium foam plasma will transfer its energy to the plasma of the main target material and heat it, thereby improving the soft X-ray (SXR) yield. A similar effect was recorded for aluminium foil with a polymer aerogel layer deposited on it [20, 21]. It is also noteworthy that a higher SXR yield was obtained for low-density bismuth than for a polished plane solid bismuth target [22]. One would also expect a similar effect from beryllium, because beryllium foam would act as a bulk absorber of laser energy [11–13], resulting in an additional increase in the total SXR yield in the case of the two-layer target. Beryllium foam would also be expected to favour smoothing out the hydrodynamic perturbations at the ablation front [12, 23–25].

The detection and identification of beryllium spectral lines in the SXR and extreme ultraviolet (EUV) regions have been the focus of numerous theoretical and experimental papers [26–34]. The choice of a radiation source in experimental works depended on the SXR wavelength region and the ionisation stage which were to be investigated. To obtain as clearly defined lines as possible and to avoid 'contamination' by higher ionisation stages, use was made as a rule of a radiation source with the lowest ion density. For the most part, the sources of radiation in these works were lamps with a hollow cathode, electrodeless discharges, arcs and sparks in gases, as well as vacuum sparks. The works dedicated to the investigation of SXR and EUV spectra of a beryllium target plasma are not numerous [35–39], the more so to the investigation of the plasma produced by a high-power nanosecond laser pulse.

An indisputable advantage of a laser-produced plasma is the possibility to obtain, in one laser pulse, X-ray spectra in a relatively broad spectral range by using the corresponding diagnostic techniques with a high spectral resolution to resolve individual spectral lines. It would appear reasonable that the line intensities in the shorter-wavelength part of SXR and EUV spectra would increase with plasma temperature [40]. For the parameters of laser radiation used in our experiments, the highest-intensity lines would be expected to be in the SXR range [37].

The earlier series of experiments with targets of low-density volume-structured materials exposed to laser radiation with broad frequency and angular spectra revealed several advantages of such radiation in comparison with the traditionally employed high-coherence radiation [41, 42]. In this connection, the investigation of SXR spectra of solid beryllium plasmas produced by laser radiation with broad frequency and angular spectra at a focal-spot intensity of $\sim10^{13}$ W cm^{-2} is a topical task. Subsequent similar investigations with beryllium foam targets of different thickness and specific density will make it possible to compare the SXR line intensities between themselves and with the data obtained with solid beryllium targets. This comparison will enable the determination of the optimal state and thickness of beryllium layer to be deposited on a heavier material of a two-layer target in the solution of laser fusion problems.

A.T. Sahakyan, S.N. Andreev, A.A. Kologrivov, T.T. Kondratenko, V.N. Puzyrev, A.N. Starodub, I.Yu. Tolstikhina, A.A. Fronya, O.F. Yakushev Lebedev Physical Institute, Russian Academy of Sciences, Leninsky prosp. 53, 119991 Moscow, Russia;
e-mail: sahakyanat@lebedev.ru

Received 9 December 2019; revision received 30 January 2020
Kvantovaya Elektronika **50** (6) 603–607 (2020)
Translated by E.N. Ragozin

2. Experimental results

Our investigations were performed on the Kanal-2 facility using a neodymium glass laser with a wavelength of 1.06 μm, a FWHM pulse duration of 2.5 ns, about ~1000 transverse modes in the oscillator, an output spectral width of ~26 Å, and a nominal radiation divergence of 1.4 mrad. The main virtues of this laser are (i) the capability to control the intensity distribution and suppress coherent perturbations in the laser focal spot simply by changing the coherence of the initial radiation in the cavity, which provides a more uniform target irradiation; (ii) a high output energy for a relatively small facility [43]. Another advantage consists in the capability to suppress small-scale focusing in the amplifier system without the use of spatial filtering. This entails a significant simplification of the laser setup and a loss reduction, and eventually improves the amplifier system efficiency and the overall laser efficiency.

Our investigations were carried out in the laser pulse energy range $W = 13-30$ J and an intensity $I = (2.3-5.3) \times 10^{13}$ W cm^{-2} at the target. For a target, we used solid Be plates. To record SXR and EUV spectra, we employed a GIS-S grazing-incidence spectrometer with an off-Rowland spectrum recording geometries, a high spectral resolution (0.3 Å), and a broad operating range (20–600 Å) (SXR + EUV). The spectra were recorded using a high-sensitivity detector with a Toshiba 1304 AP CCD linear array: 3600 pixels, an active array length of 29 mm, a pixel height of 200 μm, a pixel width of 8 μm, and an active pixel width of 6 μm. A layer of R-43 phosphor (three layers of granules 3 μm in size for a total thickness of ~10 μm) was deposited on the sensitive array elements. The spectra were identified proceeding from the data of Refs [44, 45].

Figure 1 shows the emission spectra of beryllium plasma for $W = 13$ J ($I = 2.3 \times 10^{13}$ W cm^{-2}), 20 J (3.5×10^{13} W cm^{-2}), and 30 J (5.3×10^{13} W cm^{-2}) in different ranges. In the range 20–53 Å the signal was at a noise level, and therefore this range is not depicted in the drawing. From Figs 1a and 1b it follows that the spectrum above 100 Å exhibit only the high orders of the previous lines of beryllium spectrum from the 50–100 Å range. In reality, the beryllium lines arising from longer-wavelength transitions are present in our spectra, but their intensities are much lower (several tens in the arbitrary units) than the intensity of the 1s–2p line of Be IV for a laser pulse energy of 30 J, with the result that they do not stand out against the noise background on the ordinate scale. Although we tried to use beryllium of the highest purity, the spectrum also shows a single line of oxygen (O VI). Other lines of oxygen may also make an insignificant contribution to the amplitudes of some beryllium lines.

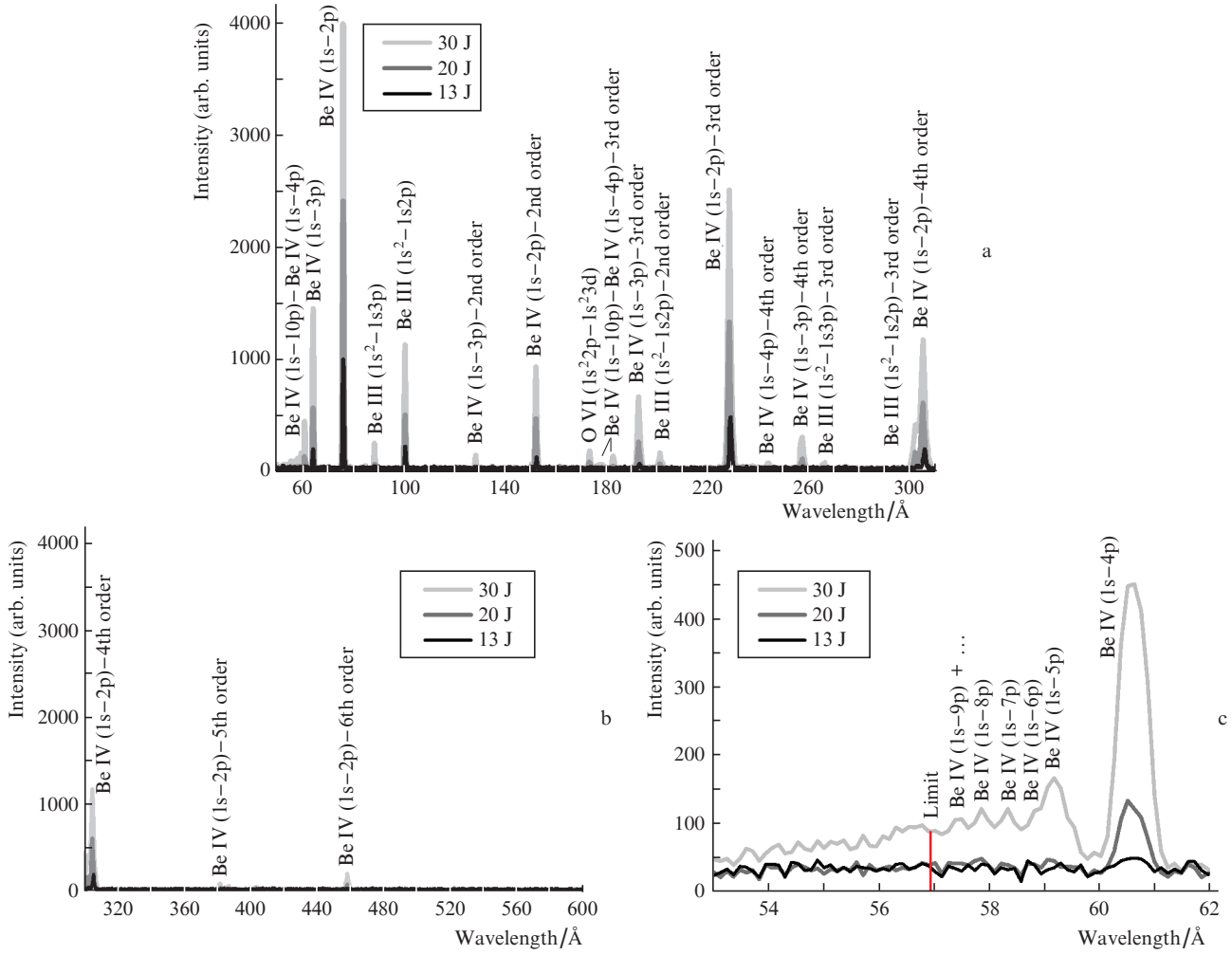

Figure 1. Emission spectra of beryllium plasma in (a) 50–310 Å, (b) 310–600 Å, and (c) 53–62 Å ranges for a laser pulse energy $W = 13$, 20, and 30 J.

Figure 1c depicts the initial portion of the spectrum in a range of 53–62 Å. One can see that the difference in the spectra with increasing pulse energy from 20 to 30 J manifests itself beginning with 54 Å: there emerges a continuous spectrum and lines Be IV (1s–5p) – Be IV (1s–9p), and maybe lines of higher-energy transitions, since their production requires less energy than the continuum. Unfortunately, the spectral resolution of our spectrograph does not permit resolving the lines Be IV (1s–9p) – Be IV (1s–15p).

It should be taken into account that the upper energy levels are collisionally depopulated in a dense plasma, with the result that some lines, from Be IV (1s–15p) and below, may not exist at all [46]. Plotted in Fig. 2 is the dependence of the limiting excited level number n^* on the particle density N and the positive ion charge Z in the plasma estimated according to Ref. [46]. One can see that the number of the limiting excited level lowers with increasing particle density. For hydrogen-like beryllium ions ($Z = 4$) for $N = 10^{20}$ cm^{-3}, the limiting excited level $n^* = 12$. For helium-like ions ($Z = 3$) $n^* = 10$. Therefore, for $N = 10^{20}$ cm^{-3} there occurs devastation of at least three upper levels under the operating conditions of Ref. [45], while the uppermost level for beryllium in Ref. [44] is Be IV (1s–10p).

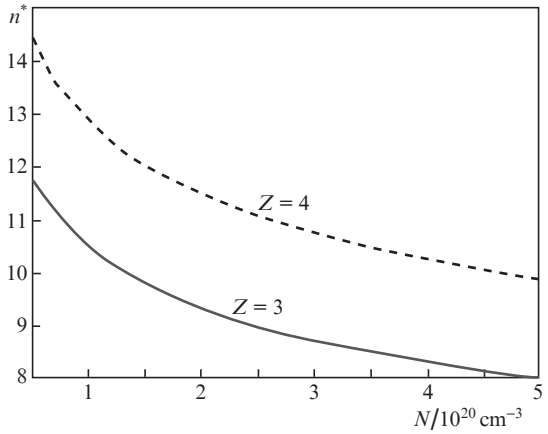

Figure 2. Dependence of the number n^* of the limiting excited level on the particle density N for positive ions of charge $Z = 3$ and 4 in the plasma.

Where comparison with the data of other works is involved, unfortunately we have not found the works concerned with the investigation of SXR beryllium plasma spectra excited by the radiation of a neodymium glass laser. The spectra obtained in Ref. [39] were found to be the closest: use was made of a solid-state laser with a pulse duration of 18 ns and an energy of about 1.5 J, and the spectra were recorded by absorption spectroscopy. In other work by the same authors [37], use was made of a ruby laser with a pulse duration of 14 ns and an energy of up to 10 J. They obtained spectra containing an intense continuum in the initial part of the SXR range without good extraction of the line spectrum, which may be attributable not only to the presence of the continuum, but also to the zero-order radiation in the recording of the spectrum. However, in both works the spectra were investigated in the direction parallel to the plane target and orthogonal to the exciting radiation, while the spectrograph in our experiments was arranged in the backward direction relative to the direction of laser radiation propagation.

To model the SXR spectra of the beryllium plasma, simulations were made using the INDHAUS programme [47, 48] (Python programming language). Its main capabilities (and advantages over other existing programmes for spectra simulations) are: (i) simulation of the spectra for any ion, electron temperature, and density; (ii) inclusion of an arbitrary number of ions of different ionisation stages; (iii) realisation of different modes of plasma behaviour (coronal limit, thermodynamic equilibrium, intermediate regimes); (iv) employment of the radiative and collisional characteristics calculated by the multiconfiguration Dirac–Fock (FAC) method; (v) the possibility of obtaining spectra with any resolution; and (vi) the possibility to work on any platform (Unix, Windows, etc.). An important advantage of the INDHAUS programme is the property specified in item (iv), because the majority of collisional-radiative models employ hydrogen-like radiative and collisional characteristics. The features described above make it possible to obtain theoretical spectra, which approximate experimental ones with a high accuracy [47, 48]. To carry out simulations in the framework of the local thermodynamic equilibrium (LTE) model, use was made of the FLYCHK code [49].

Figure 3 depicts the SXR spectra of beryllium plasma simulated theoretically in the framework of the LTE model for a laser pulse energy of 30 J as well as the spectral recorded experimentally at the same energy. A good agreement between the theoretical and experimental spectra was reached for an average plasma electron temperature of 130 eV and a density of 10^{20} cm^{-3}. One can see in Fig. 3 that the majority of spectral line peaks coincide, with the exception of the lines Be IV (1s–3p), Be III (1s^2–1s5p), and Be III (1s^2–1s4p). In the experimentally obtained spectrum the amplitude of the Be IV (1s–3p) line is higher than in the simulation, while the opposite is true of the lines Be III (1s^2–1s5p) and Be III (1s^2–1s4p). The low amplitude of the lines Be III (1s^2–1s5p) and Be III (1s^2–1s4p) may be explained as follows. The energy required for the realisation of these transitions is close to the ionisation potential of Br III, with the result that electrons do not stay in these levels and transit to the free state. In this case, the ion Be III transforms to

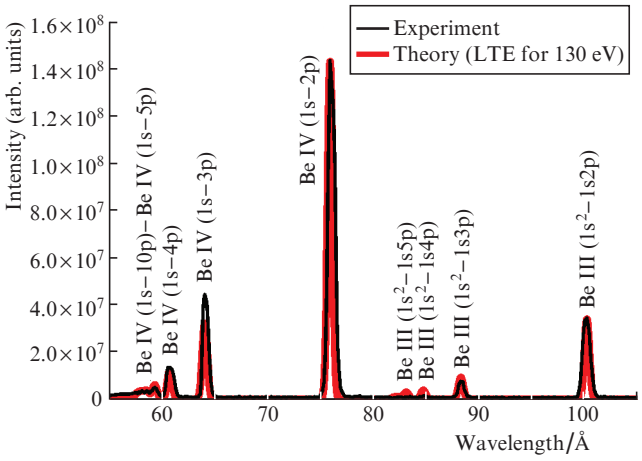

Figure 3. Theoretical and experimental emission spectra of beryllium plasma for a laser pulse energy of 30 J.

the ion Be IV excited to the state 2p and then to 3p, or directly to the state 3p. An ionisation potential of 154 eV corresponds to the production of Be IV and an ionisation potential of 218 eV corresponds to the appearance of the completely ionised ion [44]. Proceeding from the ratios of Be IV line amplitudes for different energies of laser pulses, from the presence of Be IV (1s – 5p) – Be IV (1s – 9p) lines in the spectrum for a laser intensity of 5.3×10^{13} W cm^{-2}, as well as from the dependence of the highest beryllium ion charge on the radiation intensity (Fig. 5.8 in Ref. [50]), it may be concluded that completely ionised beryllium ions are also present in the plasma.

3. Conclusions

We have obtained SXR and EUV plasma emission spectra produced by irradiating a plane solid beryllium target by 2.5-ns long pulses of laser radiation with the number of transverse modes in the oscillator ~1000 and a spectral width of ~26 Å. In the EUV range the spectral resolution was 0.3 Å. Lines up to Be IV (1s – 9p) and the plasma continuum were recorded for an on-target laser intensity of 5.3×10^{13} W cm^{-2}. The lines Be IV (1s – 10p) – Be IV (1s – 12p) may also be present in the spectrum, but the spectral resolution of our spectrograph did not permit resolving them as well as resolving them with the Be IV (1s – 9p) line. An analysis of the entire spectrum suggests that the highest-intensity part of the emission lies in the range 60 – 80 Å. For the laser intensities used in our work, the laser continuum did not manifest itself in the water window, nor even in the carbon window ranges. The SXR spectra of beryllium plasma were calculated in the framework of local thermodynamic equilibrium model using the INDAHAUS programme and the FLYCHK code. A good agreement between the simulated and experimental spectra was obtained for an average plasma electron temperature of 130 eV and an electron density of ~10^{20} cm^{-3}. When it is considered that the critical density is ~10^{21} cm^{-3} for a wavelength of 1.06 μm, for a two-layer target with the first layer made of thin porous beryllium it may be assumed that the electron density in the beryllium plasma will not be as high as ~10^{21} cm^{-3} and the laser radiation will penetrate into and simultaneously interact with the main target substance. The beryllium plasma will therefore have a favourable effect on the heating of the plasma of the main material due to collisional processes, heat exchange, and Coulomb interactions.

Acknowledgements. The authors express their appreciation to G.A. Vergunova for fruitful discussions and valuable advice.

References

1. Kreter A., Dittmar T., Nishijima D., Doerner R.P., Baldwin M.J., Schmid K. *Phys. Scr*., **T159**, 014039 (2014).
2. Doerner R.P., Baldwin M.J., Schmid K. *Phys. Scr*., **T111**, 75 (2004).
3. Doerner R.P., Baldwin M.J., Hanna J., Linsmeier Ch., Nishijima D., Pugno R., Roth J., Schmid K., Wiltner A. *Phys. Scr*., **T128**, 115 (2007).
4. Ganeev R.A., Suzuki M., Baba M., Kuroda H. *J. Opt. Soc. Am. B*, **25**, 2096 (2008).
5. Gabdullin M.T., Ramazanov T.S., Akhtanova G.B., Redmer R. *Vestnik KazNU. Ser. Fiz*., **3** (46), 3 (2013).
6. Ferro Y., Fernandez N., Allouche A., Linsmeier C. *J. Phys.: Condens. Matter*, **25**, 015002 (2013).
7. Fu Z.-G., Wang Z., Li D.-F., Kang W., Zhang P. *Phys. Rev. E*, **92**, 033103 (2015).
8. Rusu M.I., Pardanaud C., Ferro Y., Giacometti G., Martin C., Addab Y., Roubin P., Minissale M., Ferri L., Virot F., Barrachin M., Lungu C.P., Porosnicu C., Dinca P., Lungu M., Köppen M., Hansen P., Linsmeier Ch. *Nucl. Fusion,* **57**, 076035 (2017).
9. Wilson D.C., Yi S.A., Simakov A.N., Kline J.L., Kyrala G.A., Dewald E.L., Tommasini R., Ralph J.E., Olson R.E., Strozzi D.J., Celliers P.M., Schneider M.B., MacPhee A.G., Zylstra A.B., Callahan D.A., Hurricane O.A., Milovich J.L., Hinkel D.E., Rygg J.R., Rinderknecht H.G., Sio H., Perry T.S., Batha S. *J. Phys.: Conf. Ser*., **717**, 012058 (2016).
10. Tuzov Yu.V., Makrushkin Yu.E., Krasnoshchekov E.S. *VANT. Ser. Termoyadernyi Sintez*, **2**, 21 (2011).
11. Gus'kov S.Yu., Merkul'ev Yu.A. *Quantum Electron*., **31**, 311 (2001) [*Kvantovaya Elektron*., **31**, 311 (2001)].
12. Gus'kov S.Yu., Zmitrenko N.V., Popov I.V., Rozanov V.B., Tishkin V.F. *Quantum Electron*., **30**, 601 (2000) [*Kvantovaya Elektron*., **30**, 601 (2000)].
13. Borisenko N.G., Dorogotovtsev V.M., Gromov A.I., Guskov S.Yu., Merkul'ev Yu.A., Markushkin Yu.E., Chirin N.A., Shikov A.K., Petrunin V.F. *Fus. Technol*., **38**, 161 (2000).
14. Hofstetter M., Aquila A., Schultze M., Guggenmos A., Yang S., Gullikson E., Huth M., Nickel B., Gagnon J., Yakovlev V.S., Goulielmakis E., Krausz F., Kleineberg U. *New J. Phys*., **13**, 063038 (2011).
15. Bar G., Berg L., Czack G., Gras D., Haase V. *Be Beryllium: The Element. Physical Properties (continued), Electrochemical Behavior* (Berlin: Springer-Verlag, 1993).
16. Bel'kov S.A., Dolgoleva G.V., Kochemasov G.G., Mitrofanov E.I. *Quantum Electron*., **32**, 27 (2002) [*Kvantovaya Elektron*., **32**, 27 (2002)].
17. Borisenko N.G., Gromov A.I., Guskov S.Yu., Dorogotovtsev V.M., Merkul'ev Yu.A., Markushkin Ya.E., Chirin N.A., Shikov A.K., Petrunin V.F. Preprint No 62 (Moscow: Lebedev Physical Institute, 1999).
18. Wilson D.C., Bradley P.A., Hoffman N.M., Swenson F.J., Smitherman D.P., Chrien R.E., Margevicius R.W., Thoma D.J., Foreman L.R., Hoffer J.K., Goldman S.R., Caldwell S.E., Dittrich T.R., Haan S.W., Marinak M.M., Pollaine S.M., Sanchez J.J. *Phys. Plasmas*, **5**, 1953 (1998).
19. Hooper M.B. *Laser Plasma Interactions 5: Inertial Confinement Fusion* (St. Andrews: CRC Press, 1995).
20. Borisenko N.G., Akunets A.A., Khalenkov A.M., Klir D., Kmetik V., Krousky E., Limpouch J., Masek K., Merkuliev Yu.A., Pfeifer M., Pimenov V.G., Ullschmied J. *J. Rus. Laser Research*, **28**, 548 (2007).
21. Borisenko N.G., Merkuliev Yu.A. *J. Rus. Laser Research*, **31**, 256 (2010).
22. Borisenko N.G., Chaurasia S., Dhareshwar L.J., Gromov A.I., Gupta N.K., Leshma P., Munda D.S., Orekhov A.S., Tripathi S., Merkuliev Yu.A. *EPJ Web Conf*., **59**, 03014 (2013).
23. Meezan N.B., Edwards M.J., Hurricane O.A., Patel P.K., Callahan D.A., Hsing W.W., Town R.P.J., Albert F., Amendt P.A., Berzak Hopkins L.F., Bradley D.K., Casey D.T., Clark D.S., Dewald E.L., Dittrich T.R., Divol L., Döppner T., Field J.E., Haan S.W., Hall G.N., Hammel B.A., Hinkel D.E., Ho D.D., Hohenberger M., Izumi N., Jones O.S., Khan S.F., Kline J.L., Kritcher A.L., Landen O.L., LePape S., Ma T., MacKinnon A.J., MacPhee A.G., Masse L., Milovich J.L., Nikroo A., Pak A., Park H.-S., Peterson J.L., Robey H.F., Ross J.S., Salmonson J.D., Smalyuk V.A., Spears B.K., Stadermann M., Suter L.J., Thomas C.A., Tommasini R., Turnbull D.P., Weber C.R. *Plasma Phys. Control. Fusion*, **59**, 014021 (2017).
24. Simakov A.N., Wilson D.C., Yi A.A., Kline J.L., Clark D.S., Milovich J.L., Salmonson J.D., Batha S.H. *Phys. Plasmas*, **21**, 022701 (2014).
25. Yi S.A., Simakov A.N., Wilson D.C., Olson R.E., Kline J.L., Clark D.S., Hammel B.A., Milovich J.L., Salmonson J.D., Kozioziemski B.J., Batha S.H. *Phys. Plasmas*, **21**, 092701 (2014).
26. Tyrén F.Z. *Physik*, **98**, 768 (1936).
27. Edlén B. *Rep. Progr. Phys*., **26**, 181 (1963).
28. Garcia J.D., Mace J.E. *J. Opt. Soc. Am*., **55**, 654 (1965).
29. Goldsmith S. *J. Phys. B: At. Mol. Phys*., **2**, 1075 (1969).
30. Svensson L.Å. *Phys. Scr*., **1**, 246 (1970).

31. Eidelsberg M. *J. Phys. B: At. Mol. Phys*., **5**, 1031 (1972).
32. Löfstr B. *Phys. Scr*., **8**, 57 (1973).
33. Summers H.P., Dickson W.J., Boileau A., Burke P.G., Denne-Hinnov B., Fritsch W., Giannella R., Hawkes N.C., von Hellerman M., Mandl W., Peacock N.J., Reid R.H.G., Stamp M.F., Thomas P.R. *Plasma Phys. Control. Fusion*, **34**, 325 (1992).
34. Stankov B.D., Vinić M., Gavrilović Božović M.R., Ivković M. *Rev. Sci. Instrum*., **89**, 053108 (2018).
35. Langer P., Tgnon G., Dur Y., Buges J.-C. *Chronological Study of Beryllium Plasma Produced by a Laser Beam* (Essonne: Commissariat à l'énergie atomique, 1967).
36. Ariga S., Matoba T., Miyamoto K. *Jpn. J. Appl. Phys*., **12**, 484 (1973).
37. Nicolosi P., Jannitti E., Tondello G. *Appl. Phys. B*, **26**, 117 (1981).
38. Afrosimov V.V., Bobashev S.V., Golubev A.V., Simanovskii D.V., Shmaenok L.A. *JETP*, **64** (2), 284 (1986) [*Zh. Eksp. Teor. Fiz*., **91** (2), 485 (1986)].
39. Jannitti E., Nicolosi P., Tondello G. *Phys. Scr*., **36**, 93 (1987).
40. Vergunova G.A., Kologrivov A.A., Rozanov V.B., Sklizkov G.V., Shikanov A.S. *Fiz. Plazmy*, **13**, 342 (1987).
41. Fronya A.A., Borisenko N.G., Saakyan A.T., Puzyrev V.N., Starodub A.N., Yakushev O.F. *Phys. Atom. Nucl*., **82**, (10), 1 (2019); doi: 10.1134/S1063778819100090.
42. Starodub A.N., Borisenko N.G., Fronya A.A., Merkuliev Yu.A., Osipov M.V., Puzyrev V.N., Sahakyan A.T., Vasin B.L., Yakushev O.F. *Laser Part. Beams*, **28**, 371 (2010).
43. Fedotov S.I., Feoktistov L.P., Osipov M.V., Starodub A.N. *J. Rus. Laser Research*, **25**, 79 (2004).
44. Kelly R.L. *Atomic and Ionic Spectrum Lines Below 2000 Angstroms* (Tennessee: Oak Ridge National Laboratory, 1982).
45. Garcia J.D., Mack J.E. *J. Opt. Soc. Am*., **55**, 654 (1965).
46. Zel'dovich Ya.B., Raizer Yu.O. *Physics of Shock Waves and High-Temperature Hydrodynamic Phenomena* (New York: Academic Press, 1966, 1967; Moscow: Nauka, 1966).
47. Shevelko A.P., Yakushev O.F., Vainshtein L.A., Andreev S.N., Tolstikhina I.Yu. *Phys. Plasmas,* **25**, 073306 (2018).
48. Shevelko A.P., Bliss D.E., Kazakov E.D., Mazarakis M.G., McGurn J.S., Knight L.V., Struve K.W., Tolstikhina I.Yu., Weeks T.J., et al. *Plasma Phys. Rep*., **34**, 944 (2008).
49. Chung H.-K., Chen M.H., Morgan W.L., Ralchenko Y., Lee R.W. *High Energy Density Phys*., **1**, 3 (2005).
50. Anan'in O.B., Afanas'ev Yu.V., Bykovskii Yu.A., Krokhin O.N. *Lazernaya plazma: Fizika i primeneniya* (Laser Plasma: Physics and Applications) (Moscow: Izd. MIFI, 2003).